https://doi.org/10.15407/ujpe65.6.461

M.YU. TROFIMENKO,[1] S.K. ASLANOV,[1] G.S. DRAGAN,[1] V.P. SMOLYAR[2]

[1] I.I. Mechnikov Odessa National University
(2, Dvoryanskaya Str., Odessa 65082, Ukraine; e-mail: trofimenko_mikhail@ukr.net)
[2] Odessa National Polytechnic University
(1, Shevchenko Ave., Odessa 65044, Ukraine; e-mail: svp@opu.ua)

GAS FLAME STRUCTURE AND OPTICAL ASSESSMENT OF THE FLAME SPEED AND COMBUSTION EFFICIENCY

We perform the analysis of a prepared propane-butane flame structure, by using the computer processing of the radiation from the chemical reaction zone. We mark out the stoichiometric reaction along with the zones of the external oxidant inflow into the flame for different burner diameters. We suggest a method of determining the normal flame speed based on catching the moment of the complete fuel combustion in the upper part of a flame. We show a role of the external oxidant inflow in the kinetic processes within the burning zone. The absolute value of the normal component of the flame speed and its dependence on the burner diameter and on the excess oxidant ratio for a prepared propane-butane flame are determined experimentally.

K e y w o r d s: propane-butane flame, flame structure, flame speed, ambient air, flame study.

1. Introduction

The study of the hydrocarbon fuels burning mechanisms in order to increase the efficiency of their usage is still a topical problem of the contemporary power engineering, despite a rather long history of the premixed fuel combustion research. It began to attract even more interest lately in context of the internal combustion engines (ICE) development [1–3]. It is no secret that the automotive industry faces a strong pressure from the public to reduce vehicle emissions, especially in the urban areas. The major challenges for ICE science and engineering are the optimization of combustion to improve the fuel economy, lowering the pollutant emissions, and searching for new alternative fuels [1, 4]. There are various approaches to these problems, among them the study of different diluents [2–5], biofuels [1, 2], particularly, enriched with hydrogen [2, 3], soot formation and its subsequent oxidation [6], *etc.* However, the primary goal of any fundamental study of the combustion is to gain a thorough understanding of the mechanisms of ignition, species distribution, flame propagation, and energy release of combustible mixtures [7].

When dealing with the technical implementation of the combustion installations, one has to consider the turbulent flows [8] and acoustic oscillations [9, 10], which requires a special treatment. However, the properties of laminar flames are generally believed to be particularly good for the theory verification and the better understanding of the whole combustion process or its certain parameters [4, 7, 11–13]. This is largely due to the possibility of precise fixation and measurement of the most important flame properties, and the most important among them is surely the *laminar burning velocity* (often simply referred to as the *flame speed*). An accurate knowledge of this property, together with the influence of other variables on it, is important for both the validation of new kinetic models, and as an input to the calibra-

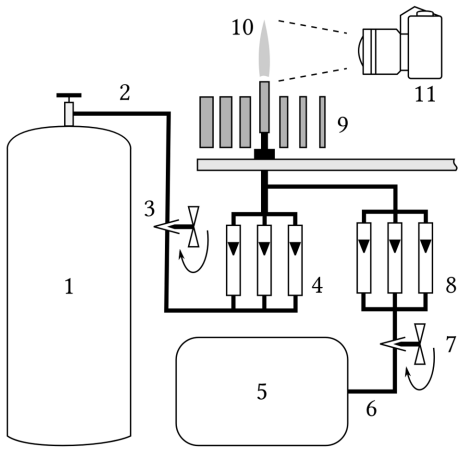

Fig. 1. Experimental setup. *1* – gas vessel; *2, 6* – pipes; *3, 7* – needle taps; *8, 4* – sets of rotameters, measuring the air and gas flows, respectively; *5* – compressor; *9* – a set of nozzles of different diameters; *10* – flame under study; *11* – video camera

tion of turbulent combustion and pollutant formation [4, 6, 7, 12]. Of course, it is of no less importance for such practical applications as internal combustion engines operating at different pressures [4].

In light of the above cited, the normal flame speed (V_n) is also considered a major indicator of the combustion efficiency, along with the maximum temperature. Therefore, numerous papers are devoted to the development and application of various methods of mixed fuel burning speed determination depending on the conditions and properties of a fuel [1, 11–16].

In particular, paper [15] gives the results of experimental measurements of the normal flame speed in various combustible mixtures, but the authors do not consider the influence of the external oxidant inflow on the burning kinetics. In order to get more reliable results, it is reasonable to use the laser methods which have no impact on the burning kinetics, thus providing a more accurate determination of the burning zone boundaries [17]. The form of the burning surface must also be taken into account [18, 19]. The air balance in the burning zone is especially important, since it affects the flame structure, kinetics of all the processes, and measured parameters [20, 21]. The authors of [22] give the calculated data on the flame speed for a number of typical gas mixtures under the pressures up to 6000 atm and temperatures up to 4000 K. They claim that the major contribution to the flame speed comes from the initial temperatures. In paper [23], a theoretical model for propane-butane burning in the air atmosphere with a diffusion burner is presented with the emphasis on burning conditions and the flame structure. The authors of [24] also conducted an experimental study of the lean propane-butane mixtures with hydrogen additions in combustion chambers with spark ignition. They used the normal flame speed to actually estimate the impact of hydrogen additions on the mixture burning.

The gas fuels best studied up to date are hydrogen and methane (which maintains its popularity as a major component of the natural gas, among others) [4, 5, 14]. These fuels are best presented in the literature. However, more experimental and kinetic model development studies are required for other fuels [11].

The propane-butane mixtures are also a popular fuel in various industrial, automotive and household applications, and often in the standardized proportion (40% propane and 60% butane) [25–28].

So the aim of this paper is to study the structure of a prepared propane-butane mixture flame utilizing the computer processing of the radiation from the burning zone in order to reveal the impact of the external oxidant and the burner form on the value of the normal flame speed.

2. Experiment

We used a setup shown in Fig. 1 in our experiments. The setup includes the fuel and oxidant supply systems with the continuous monitoring of their consumption, and a video camera for the flame radiation capture. The setup design allows us to use the replaceable nozzles with different diameters for the burner, required for obtaining different shapes of the flame. In order to guarantee the laminarity of the mixture flow, the length of the nozzles was calculated as $L_{\min} = 0.03 d\,\mathrm{Re}$ (Re is the Reynolds number, d is the changeable nozzle diameter). We also used the set of nozzles of 0.4 cm, 0.5 cm, 0.6 cm, 0.7 cm, 0.8 cm, 0.9 cm, and 1 cm in diameter (see Fig. 1). The Reynolds number did not exceed 940 throughout the experiment.

The fuel and oxidant supply system ensured their uniform mixing and maintaining the laminar flow through a burner. By changing the nozzles, we obtained the flames of different sizes. The images of flames were recorded with the Canon EOS 400D DIGITAL camera with exposure time of 1/200 s. This

camera has a 22.5×15 mm CMOS sensor reported to have a solid response in the $420 \div 680$ nm wavelength range [29].

The equality of the burning conditions is ensured, when the following requirements are met: **a)** the measurements of the normal flame speed are performed, when the closed inner cone of the flame is formed, which is accompanied by the extinction of the yellow glow from the condensed phase; this case is assumed to correspond to the complete combustion of a fuel in the upper part of the flame, and particularly, the carbon particles (Fig. 2, *a*); **b)** along with point a), the specific fuel rate U should also be kept equal for the burners of different diameters ($U = Q_{\text{tot}}/S_{\text{burner}}$, where Q_{tot} is the combustible mixture flow measured with rotameters, S_{burner} is the cross-section of a changeable upright burner).

We study the burning of the open propane-butane flame (40% propane, 60% butane) above the upright burner with the forced supply of reactants (air as an oxidant), surrounded by the air atmosphere under normal conditions (temperature 20 °C, pressure 768 mm Hg). The simplified schematic diagram of the experimental setup is shown in Fig. 1. The conditions of the experiment were chosen similar to those described in [20, 30].

The value of the normal flame speed V_n was found using the method suggested by us in [31, 32]. This method allows one to determine both the total value of V_n for the entire flame, and its distribution along the burning front.

Thus, the suggested method of experimental study of the fuel combustion efficiency is based on the determination of the normal flame speed with similar arrangement of the combustible mixture flow. The flame structure and the reached values of V_n depend on the burning process setup, namely on the fuel preparation conditions (excess oxidant ratio, mixture homogeneity, *etc.*) and the burning conditions (burner diameter, combustible mixture flow, model pipe diameter, *etc*).

3. Results and Discussion

A typical image of the Bunsen laminar flame taken under the described conditions is shown in Fig. 2, *a*. The spatial resolution of such images was usually between 250 and 300 pixels/cm. With an absolute measurement error of 3 pixels, it yields the length error of about 0.01 cm.

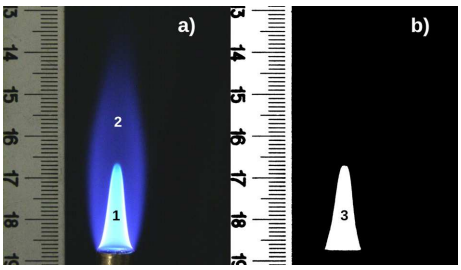

Fig. 2. An example of the flame image taken under the conditions described in the text (*a*); a digitally binarized monochromatic representation of the photographic image (*a*) with certain brightness threshold (*b*); *1* – inner cone of the Bunsen flame; *2* – outer cone of the Bunsen flame; *3* – a separated silhouette of the inner cone ready for the automated radius measurements and further processing

The studied flame is a typical shaped Bunsen flame consisting of two cones – the inner cone (zone 1 in Fig. 2, *a*) and the outer cone (zone 2 in Fig. 2, *a*) divided by a bright border – the burning front. The heating and the pre-burning preparation of the combustible mixture happen within the inner cone, while the after-burning takes place in the outer cone.

According to the method [31], in order to determine V_n from the flame images, we applied some digital image processing first. We binarized the images with certain brightness threshold basing on the sum of the RGB channels. In this way, we obtained a silhouette image of the inner cone bounded by the burning front (zone 3 in Fig. 2, *b*). Next, by measuring the radius R at each height, we calculated the lateral surface in the conic frustum approximation.

We conducted the similar procedures for different burner diameters under the conditions (*a*) and (*b*) mentioned in the previous section. The resulting images are shown in Fig. 3.

As seen from this figure, with different diameters, conditions (*a*) and (*b*) hold true at different oxidant-to-fuel ratios. The dependences of the excess oxidant ratio α in the initial combustible mixture on the burner diameter are shown in Fig. 4. The form of the open propane-butane flames is determined by the interaction of the fuel with the oxygen supplied from two sources. The *first* source is the oxygen contained in the initial combustible mixture coming from the burner and controlled by the rotameter readings. The *second* source is the oxygen from the ambient air, the amount of which is determined by the suction from outside. So, the introduced condition a) is fulfilled

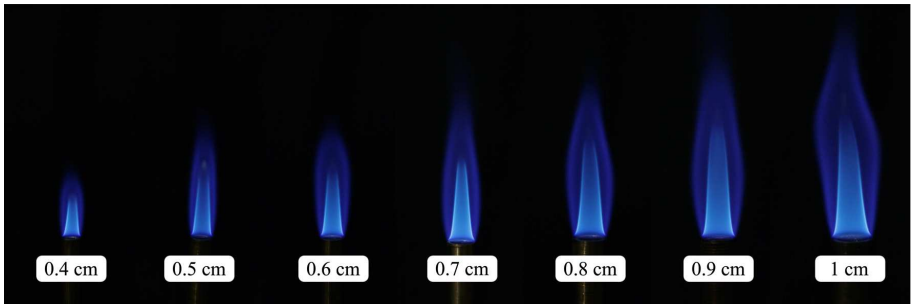

Fig. 3. Photographic images of the flames for the burners of different diameters

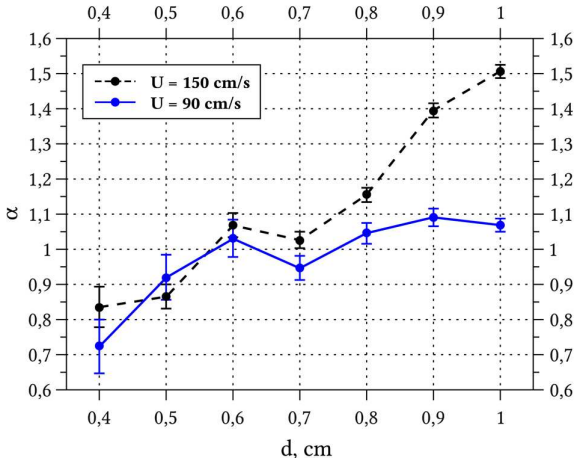

Fig. 4. Dependence of α on the burner diameter

by the excess oxidant ratio $\alpha' = \frac{Q_{\text{a.m.}}+Q_{\text{a.n.}}}{27.38\,Q_g}$, where $Q_{a.m.}$ is the amount of air in the initial mixture determined with a rotameter, $Q_{\text{a.n.}}$ is the amount of the secondary (ambient) air, Q_g is the amount of a gas in the initial mixture determined with a rotameter. So, the value α' is larger than α of the initial mixture $\alpha = \frac{Q_{\text{a.m.}}}{27.38\,Q_g}$ calculated from the rotameter readings.

The value of α and the uncertainty σ_α were estimated from the expression:

$$\alpha = \frac{a\,Q_{\text{air}}}{b\,Q_{\text{gas}}} \pm \sigma_\alpha, \tag{1}$$

$$\sigma_\alpha = \frac{a}{b}\sqrt{\left(\frac{\sigma_{\text{air}}}{Q_{\text{gas}}}\right)^2 + \left(\frac{Q_{\text{air}}\sigma_{\text{gas}}}{Q_{\text{gas}}^2}\right)^2}, \tag{2}$$

where Q_{air} is the air flow rate, Q_{gas} is the gas flow rate, $\sigma_{\text{air}} \sim 1$ cm^{3}s^{-1}, $\sigma_{\text{gas}} \sim 0.025$ cm^{3}s^{-1} are the uncertainties of the air and gas flows, respectively, $a = 0.21$ is the portion of oxygen in the atmospheric air, $b = 5.9$ is the number of oxygen molecules required for the oxidation of an average molecule in the propane+butane mixture (40% propane, 60% butane).

Apparently, in the case of $U = 150$ cm/s, the obtained dependence of α on the diameter (corresponding to the conditions (a) and (b), as before) may be explained by the reducing role of the ambient air and the necessity to compensate it with the primary air in the initial combustible mixture.

In the case of $U = 90$ cm/s, the duration t ($t = l/U$, where l is the flame height) of the pre-burning preparation of the selected elementary volume is greater than in the case of $U = 150$ cm/s, and the pre-burning decomposition of the combustible mixture is deeper. All this leads to an increase in the role of kinetic reactions (near the burning front). Starting from a certain diameter (0.6–1 cm), the energy gain from the increased role of kinetic reactions grows, which promotes a more complete combustion and compensates a decrease of the secondary air amount.

The total flame speed V_n was estimated from the expression:

$$V_n = \frac{Q_{\text{air}} + Q_{\text{gas}}}{S}, \tag{3}$$

where S is the optically measured area of the burning front surface (see Fig. 2). As each mode of combustion was photographed several times, the resultant uncertainty may be estimated from the relation:

$$\frac{1}{N}\sqrt{\sigma_{V(\text{meas})}^2 + \sigma_{V(\text{rand})}^2}, \tag{4}$$

where N is a number of images for each combustion mode, $\sigma_{V(\text{rand})}$ is the random V_n error taking the Student coefficient into account for the 95% confidence interval; $\sigma_{V(\text{meas})}$ is the measurement error defined as

$$\sigma_{V(\text{meas})} = \sqrt{(\sigma_Q/S)^2 + (Q\,\sigma_S/S^2)^2}, \tag{5}$$

and, according to the experimental conditions and the method [30],

$$\sigma_Q \approx \sigma_{\text{air}}, \quad \sigma_S = \sqrt{H\,(2\pi R\sigma_R)^2}, \tag{6}$$

where H is the flame height in pixels, R is the mean radius of the corresponding flame, and σ_R is the linear size measurement error equivalent to 3 pixels in the image. A typical value of $\sigma_R \sim 0.01$ cm.

The obtained dependences of the normal flame speed on the nozzle diameter are shown in Fig. 5. The quantity of interest is apparently significantly larger than the measurement error, which confirms the applicability of the chosen optical approach. Just as for the dependence of α on the burner diameter, we conducted the experiments for two different values of the fuel rate U: $U_1 = 150$ cm/s and $U_2 = 90$ cm/s. The forms of the measured dependences happen to be almost identical. The relative supply of the ambient air is large for small diameters, and the boundary of the inner cone is located near the burning front. With small diameters (0.4–0.5 cm), the gas at the inner cone border burns at larger values of α (because of the outer air), and a layer with a reduced proportion of the gas as compared with the value averaged over the flame is formed. The impact of the outer air reduces with the diameter, and the flame speed reaches larger values (at 0.6–0.7 cm). Starting with a certain diameter, the role of the ambient air drops almost entirely, and V_n decreases (0.7–1 cm). Therefore, it is not only the total amount of air participating in the reaction that matters, but it is also the geometric place of its supply.

The V_n dependence on α for the burners of different diameters is shown in Fig. 6. The growth of V_n with α is observed for all the studied diameters. All the curves reach the maximum at certain values of α, which depend on the specific mixture flow. For example, for a diameter of 0.5 cm, the experiment conditions predetermine a high specific mixture flow, a small time in the flame, and a significant heat outflow.

As was noted in [33], under the rotating electric field due to the mixing intensification, the flame height tends to decrease by 18–20%, while preserving the total emission of radiation at the wavelengths of CH, C_2, and OH radicals. In [20, 30], it was also noted that the flame height may decrease with the pulsating burning onset at some values of α, which is accompanied by the higher temperature and combustion completeness.

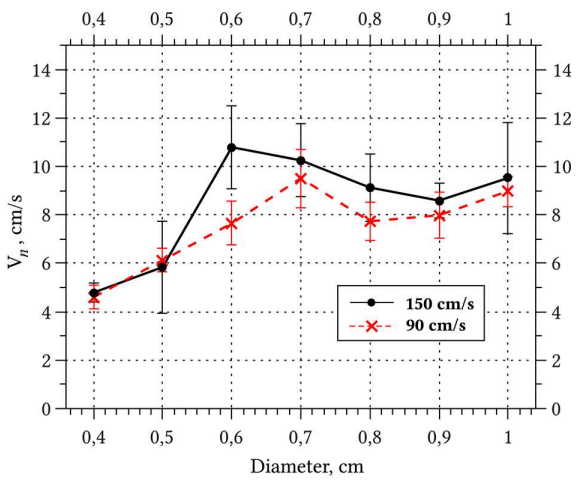

Fig. 5. V_n dependence on the flame diameter

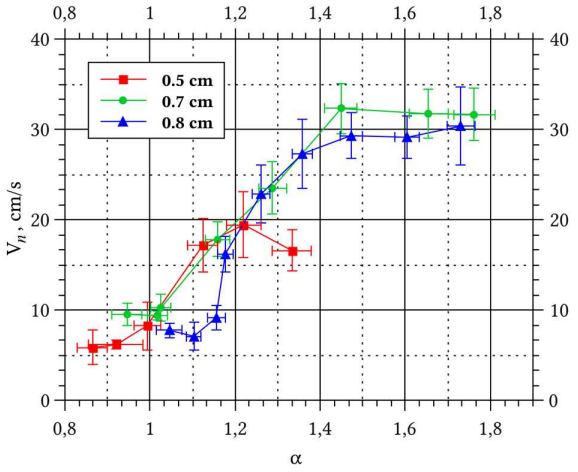

Fig. 6. V_n dependence on α for different diameters

In both cases (the electric action and the pulsating burning), the processes taking place in a flame lead to the extra mixing of reactants within the inner cone, better pre-burning preparation, and increased kinetic component of the reaction. This leads, in turn, to the higher temperature and size of the heated zone inside the inner cone.

The higher temperatures may be achieved, by adjusting the pre-mixed fuel in order to restructure the flame geometry in such a way that the maximum temperatures become higher [20,30], corresponding to the higher electrical breakdown voltage at the same time [20]. This corresponds to higher flame speeds in our measurements and may be seen in Fig. 6.

So, a decrease of the inner cone size, while maintaining α and the total mixture flow, indicates more intense reactions, higher V_n, and the more efficient combustion.

4. Summary and Conclusions

From the conducted experiment, we observe that, as the burner diameter increases, the time for the elementary volume to stay within the flame increases, which results in the better pre-burning preparation and (as mentioned before) the increased role of the kinetic reaction component. The values of V_n also increase. For a fixed diameter, the flame height decreases for greater α, just as in [31], so V_n grows. Starting at certain values of α, the V_n dependence on α reaches its maximum and then gradually falls till the extinction, supported only by a more complete combustion and the increased role of kinetic reactions.

The formation of the closed inner cone in the flame is driven by two processes: the secondary (outer) air supply to the flame, and the heat balance within the inner cone volume. For the small diameters of the burner (and consequently, the small inner cone), the major part is the secondary air supply, which may lead to the insufficient fuel at the burning front. The linear size (and the total surface) of the burning front may increase in this case, which would correspond to smaller V_n.

For larger diameters, the inner cone structure is determined by the processes within the central area bounded by the burning front. The heat balance between its diffuse outflow and the generation by burning reactions shifts toward the heat accumulation within the inner cone. This makes the heat zone larger and the pre-burning preparation better – through the increased role of the kinetic reactions in the flame.

1. L. Pizzuti, C.A. Martins, P.T. Lacava. Laminar burning velocity and flammability limits in biogas: A literature review. *Renewable and Sustainable Energy Reviews* **62**, 856 (2016).
2. Roopesh Kumar Mehra, Hao Duan, Romualdas Juknelevičius, Fanhua Ma, Junyin Li. Progress in hydrogen enriched compressed natural gas (HCNG) internal combustion engines – a comprehensive review. *Renewable and Sustainable Energy Reviews* **80**, 1458 (2017).
3. A. Sofianopoulos, D.N. Assanis, S. Mamalis. Effects of hydrogen addition on automotive lean-burn natural gas engines: Critical review. *J. Energy Engineering* **142**, E4015010 (2016).
4. Panfeng Han, M. David Checkel, Brian A. Fleck, Natalie L. Nowicki. Burning velocity of methane/diluent mixture with reformer gas addition. *Fuel* **86**, 585 (2007).
5. A.N. Mazas, D.A. Lacoste, T. Schuller. Experimental and numerical investigation on the laminar flame speed of CH_4/O_2 mixtures diluted with CO_2 and H_2O. In: *Proceedings of ASME Turbo Expo 2010: Power for Land, Sea and Air GT2010* (ASME, 2010).
6. B.R. Stanmore, J.F. Brilhac, P. Gilot. The oxidation of soot: A review of experiments, mechanisms and models. *Carbon* **39**, 2247 (2001).
7. C.J. Rallis, A.M. Garforth. The determination of laminar burning velocity. *Progress in Energy and Combustion Science* **6**, 303 (1980).
8. D.B. Spalding. Mathematical models of turbulent flames; A review. *Combust. Sci. Techn.* **13**, 3 (1976).
9. T. Lieuwen. Modeling premixed combustion-acoustic wave interactions: A review. *J. Propulsion and Power* **19**, 5 (2003).
10. V.V. Golub, D.I. Baklanov, S.V. Golovastov, K.V. Ivanov, M.F. Ivanov, A.D. Kiverin, V.V. Volodin. Influence of an acoustic field on flame development and transition to detonation. *High Temp* **48**, 860 (2010).
11. Alexander A. Konnov, Akram Mohammad, Velamati Ratna Kishore, Nam Il Kim, Chockalingam Prathap, Sudarshan Kumar. A comprehensive review of measurements and data analysis of laminar burning velocities for various fuel+air mixtures. *Progress in Energy and Combustion Science* **68**, 197 (2018).
12. Oras Khudhair, Haroun A.K. Shahad. A review of laminar burning velocity and flame speed of gases and liquid fuels. *Int. J. Current Engin. Technol.* **7**, 183 (2017).
13. F.N. Egolfopoulos, N. Hansen, Y. Ju, K. Kohse-Höinghaus, C.K. Law, F. Qi. Advances and challenges in laminar flame experiments and implications for combustion chemistry. *Progress in Energy and Combustion Science* **43**, 36 (2014).
14. G.E. Andrews, D. Bradley. Determination of burning velocities: A critical review. *Combustion and Flame* **18**, 133 (1972).
15. Yu.V. Polezhaev, I.L. Mostinskii. The normal flame velocity and analysis of the effect of the system parameters on this velocity. *High Temperature* **43**, 937 (2005).
16. Yu.N. Shebeko, A.Yu. Shebeko. About the constancy of the normal burning velocity of gaseous mixtures near flammability limits in gases. *Fire Safety* **2**, 106 (2014) (in Russian).
17. A. Popov, A. Tyurin, V. Tkachenko, A. Bekshaev, V. Kalinchak, M. Trofimenko. Speckle-interferometric approach to flame diagnostics. In: *Imaging and Applied Optics 2015*, OSA Technical Digest (Optical Society of America, 2015), paper JT5A.43.
18. V.V. Kalinchak, F.F. Karimova, S.G. Orlovskaya, M.S. Shkoropado. Image processing for determination of the flame speed. In: *16th International Conference "Digital Signal Processing and its Applications" (DSPA-2014), 2014* (March 26–28, 2014 Moscow, Russia).

19. Irvin Glassman, Richard A. Yetter. *Combustion* (Academic Press, 2008).
20. M.Yu. Trofimenko, S.K. Aslanov, V.P. Smolyar. Electrical structure of the jet of a gas mixture flame. *Surface Engineering and Applied Electrochemistry* **50**, 275 (2014).
21. Zhenyan Guo, Yang Song, Qun Yuan, Tuya Wulan, Lei Chen. Simultaneous reconstruction of 3D refractive index, temperature, and intensity distribution of combustion flame by double computed tomography technologies based on spatial phase-shifting method. *Optics Communications* **393**, 123 (2017).
22. A.A. Vasiliev, A.V. Trilis. Velocity of deflagration combustion at high pressures and temperatures. *Thermophysics and Aeromechanics* **20**, 605 (2013).
23. V.Yu. Polshikov. Mathematical model of the propane-butane mixture burning under deficiency in oxidizer in diffusion burner. in *Proceedings of the International scientific conference (Chita, April 2012)* (Molodoi Uch. Publ., 2012), pp.130-133. (in Russian)
24. E.A. Fedyanov, E.A. Zakharov, Y.V. Levin, D.S. Gavrilov. Experimental study of combustion of propane-butane-air mixture with addition of hydrogen. *Bulletin of Saratov State Technical University* **11**, 104 (2013) (in Russian).
25. Yu.P. Kluchka, A.I. Tarariev. Analysis of fire and explosion hazard in the propane-butane gas storage system. *Questions of Fire Safety* **34**, 98 (2013) (in Russian).
26. A.I. Grushevskiy, A.S. Kashura, A.I. Blyankinshtein, E.S. Volodin, A.M. Askhabov. *Ecological Properties of the Automotive Operational Materials* (Siberian Federal Univ., 2015) (in Russian).
27. GOST 27578-87 "Liquefied hydrocarbon gases for motor transport. Specifications".
28. GOST 20448-90 "Liquefied hydrocarbon fuel gases for domestic use. Specifications".
29. V. Lebourgeois, A. Bégué, S. Labbé, B. Mallavan, L. Prévot, B. Roux. Can commercial digital cameras be used as multispectral sensors? A crop monitoring test. *Sensors* **8**, 7300 (2008).
30. M.Yu. Trofimenko, S.K. Aslanov, V.P. Smolyar. Structural changes in the gas flame upon the pulsating combustion mode onset. *Ukr. J. Phys.* **59**, 359 (2014).
31. M.Yu. Trofimenko, S.K. Aslanov, G.S. Dragan, V.P. Smolyar. The normal component of a gas flame speed. *Ukr. J. Phys.* **62**, 214 (2017).
32. M.Yu. Trofimenko, S.K. Aslanov, A.Ya. Bekshaev, V.P. Smolyar. Optical determination of the normal component of the gas flame speed. In *Proceedings of the 7th IEEE International Conference on Advanced Optoelectronics and Lasers, CAOL 2016* (Odessa; Ukraine, 2016), Article number 7851389.
33. A.V. Tupikin, P.K. Tretyakov, N.V. Denisova, V.V. Zamashchikov, V.S. Kozulin. Diffusion flame in an electric field with a variable spatial configuration. *Combustion, Explosion, and Shock Waves* **52**, 167 (2016).

Received 26.01.18

М.Ю. Трофименко, С.К. Асланов,
Г.С. Драган, В.П. Смоляр

СТРУКТУРА ГАЗОВОГО ПОЛУМ'Я І ОПТИЧНА ОЦІНКА ШВИДКОСТІ ГОРІННЯ ТА ЕФЕКТИВНОСТІ СПАЛЮВАННЯ

Р е з ю м е

В роботі проведено аналіз структури попередньо підготовленого пропан-бутанового полум'я методом комп'ютерної обробки випромінювання зони хімічної реакції. Виявлено області стехіометричної реакції та підсмоктування зовнішнього окисника у факелі при різних діаметрах пальника. Запропоновано методику визначення нормальної швидкості горіння, засновану на фіксації моменту повного згоряння палива у верхній зоні факела. Показано роль підсмоктування зовнішнього окисника в кінетичних процесах у зоні горіння. Експериментально визначено абсолютні значення та залежності величин нормальної складової швидкості горіння попередньо підготовленого пропан-бутанового полум'я в залежності від діаметра факела та коефіцієнта надлишку окисника в пальній суміші.